

Effects of Zeeman degeneracy on the steady-state properties of an atom interacting with a near-resonant laser field: Probe spectra

Bo Gao

2414 John R Road, Apt. 206, Troy, Michigan 48083

(Received 3 June 1993)

The probe spectrum of a closed two-level Zeeman-degenerate atom interacting with a linearly polarized coherent laser field is studied. Results for the cycling transition of a cesium atom are presented and compared to the experimental data of Lounis *et al.* [Phys. Rev. Lett. **69**, 3029 (1992)]. We further show that the resonance derived by Grynberg, Vallet, and Pinard [Phys. Rev. Lett. **65**, 701 (1990)] is due to stimulated Raman scattering.

PACS number(s): 32.70.-n, 32.80.Pj, 42.65.Dr

The aim of this paper is to study the effects of Zeeman degeneracy on the probe spectrum of an atom interacting with a linearly polarized coherent laser field. It is motivated largely by original experiments on the probe spectra of cold atoms trapped by three orthogonal pairs of counterpropagating σ^+ - σ^- laser beams [1,2]. These experiments uncovered narrow structures (much narrower than the spontaneous decay width) which are subsequently interpreted as results of stimulated Raman processes among ground-state Zeeman sublevels [2]. Recently, a similar experiment [3] has been carried out in a one-dimensional (1D) σ^+ - σ^- optical molasses configuration, making it even more attractive for a theoretical treatment. Existing theories [3-5] show good qualitative agreement with the experiment. Quantitative

comparison has, however, not been possible because the level structures of the cycling transition of the cesium atom, with $F_g=4$ and $F_e=5$, were modeled as a 1 to 2 transition. Here we present a theory that treats transitions with arbitrary angular momentum, detuning, and Rabi frequency easily and efficiently. Absolute cross sections with no fitting parameters will be presented for the cycling transition of Cs and compared to the experimental data [3]. Atomic motion will, however, be ignored, and as a result the Rayleigh [3,5] and the recoil resonances [4,5] will be missed.

The derivation of the probe spectrum for an atom in a coherent laser field is very similar to the derivation of the resonance fluorescence spectrum presented in [6]. I will simply give the result for a stationary atom

$$\sigma_e(\omega) = \left[\frac{4\pi\omega_{eg}}{\hbar c} \right] \lim_{\eta \rightarrow 0^+} \text{Re} \{ \text{Tr}_A (\mathbf{e}^* \cdot \boldsymbol{\mu}^-) R(\eta - i(\omega - \omega_L)) [\rho_A^{\text{SS},R}(\mathbf{e} \cdot \boldsymbol{\mu}^+) - (\mathbf{e} \cdot \boldsymbol{\mu}^+) \rho_A^{\text{SS},R}] \} . \quad (1)$$

Here σ_e is the net gain cross section for probe photons with polarization \mathbf{e} . $\boldsymbol{\mu}^\pm$ are the atomic raising and lowering dipole operators, respectively. $R(s)$ is the resolvent operator defined by $R(s) \equiv [s - L_A^R]^{-1}$ in which L_A^R is the Liouville operator defined by the density-matrix equation (in the rotating frame) for an atom in the pump laser field and $\rho_A^{\text{SS},R}$ is the corresponding steady-state solution. Assuming linear polarization and taking the pump polarization as the quantization axis, we have [7,8]

$$\begin{aligned} \partial_t \rho_A^R(t) &\equiv L_A^R \rho_A^R(t) \\ &= -i \left\{ \left[-(\Delta + i\gamma/2) \sum_{m_e} |J_e m_e\rangle \langle J_e m_e| \right] \rho_A^R(t) - \rho_A^R(t) \left[-(\Delta + i\gamma/2) \sum_{m_e} |J_e m_e\rangle \langle J_e m_e| \right]^\dagger \right\} \\ &\quad + \gamma \sum_{q, \text{all } m} \langle J_g m_g' 1q | J_e m_e' \rangle |J_g m_g'\rangle \langle J_e m_e' | \rho_A^R(t) |J_e m_e\rangle \langle J_g m_g | \langle J_g m_g 1q | J_e m_e \rangle \\ &\quad - i \left[-(\Omega_{eg}/2) \sum_m f_m (|J_e m\rangle \langle J_g m| + |J_g m\rangle \langle J_e m|), \rho_A^R(t) \right], \end{aligned} \quad (2)$$

where $\Delta = \omega_L - \omega_{eg}$ is the laser detuning, γ is the spontaneous decay rate of the excited state, $\Omega_{eg} = E_0 \langle J_e || \boldsymbol{\mu} || J_g \rangle / \hbar$ is the reduced Rabi frequency, and

$$f_m \equiv (-1)^{J_e - m} \begin{bmatrix} J_e & 1 & J_g \\ -m & 0 & m \end{bmatrix} .$$

J is here merely a notation that can also stand for F . In deriving Eq. (1), the probe field is treated only to the first order in perturbation theory. The processes it describes involve therefore one and only one probe photon.

It is convenient to define $\sigma_q \equiv \sigma_{e=\epsilon_q}$ where $\epsilon_0 = \hat{z}$; $\epsilon_1 = -(1/\sqrt{2})(\hat{x} + \hat{y})$, and $\epsilon_{-1} = (1/\sqrt{2})(\hat{x} - \hat{y})$. They can then be written as

$$\begin{aligned} \sigma_0(\omega) = & 3(2J_e + 1)\gamma \sum_{mm'} f_m f_{m'} \text{Re} \{ [\langle m | R_{eg,gg}^{(0)}(-i(\omega - \omega_L)) | m' \rangle - \langle m | R_{eg,ee}^{(0)}(-i(\omega - \omega_L)) | m' \rangle] \langle J_g m' | \rho_A^{SS,R} | J_e m' \rangle \\ & + \langle m | R_{eg,eg}^{(0)}(-i(\omega - \omega_L)) | m' \rangle \\ & \times [\langle J_e m' | \rho_A^{SS,R} | J_e m' \rangle - \langle J_g m' | \rho_A^{SS,R} | J_g m' \rangle] \} [\pi(\lambda_{eg}/2\pi)^2]; \end{aligned} \quad (3)$$

$$\begin{aligned} \sigma_1(\omega) = & 3(2J_e + 1)\gamma \sum_{mm'} h_m h_{m'} \text{Re} \{ \langle m | R_{eg,gg}^{(1)}(-i(\omega - \omega_L)) | m' \rangle \langle J_g m' | \rho_A^{SS,R} | J_e m' \rangle \\ & - \langle m | R_{eg,ee}^{(1)}(-i(\omega - \omega_L)) | m' \rangle \langle J_g m' - 1 | \rho_A^{SS,R} | J_e m' - 1 \rangle \\ & + \langle m | R_{eg,eg}^{(1)}(-i(\omega - \omega_L)) | m' \rangle \\ & \times [\langle J_e m' | \rho_A^{SS,R} | J_e m' \rangle - \langle J_g m' - 1 | \rho_A^{SS,R} | J_g m' - 1 \rangle] \} [\pi(\lambda_{eg}/2\pi)^2]; \end{aligned} \quad (4)$$

and $\sigma_{-1}(\omega) = \sigma_1(\omega)$ in the absence of any magnetic field. Here $\rho_A^{SS,R}$ is the steady-state solution of Eq. (2) for which simple analytic formulas were derived in [8],

$$h_m \equiv (-1)^{j_e - m} \begin{bmatrix} J_e & 1 & J_g \\ -m & 1 & m-1 \end{bmatrix},$$

and λ_{eg} is the wavelength of the atomic transition. We have also defined

$$\langle m | R_{ab,cd}^{(l)}(s) | m' \rangle \equiv \langle \langle am, bm - l | R(s) | cm', dm' - l \rangle \rangle, \quad (5)$$

which can be calculated easily for any transition using the method of [8]. σ_q so defined is associated with processes in which one probe photon with polarization q is involved. It is therefore clear that stimulated Raman processes contribute only to $\sigma_{\pm 1}$, and stimulated Rayleigh processes contribute only to σ_0 .

The gain cross section for a weak probe of arbitrary polarization and arbitrary direction of propagation can be related easily to $\sigma_q(\omega)$ by straightforward angular-momentum algebra. For example, the cross section for a linearly polarized probe beam is given in general by

$$\sigma(\omega, \theta) = \cos^2(\theta)\sigma_0(\omega) + \sin^2(\theta)\sigma_1(\omega), \quad (6)$$

where θ is the angle between the polarizations of the probe and the pump lasers. Similarly the cross section for a circularly polarized (either + or -) probe beam can be written in general as

$$\sigma(\omega, \theta) = \frac{1}{2} \sin^2(\theta)\sigma_0(\omega) + \frac{1}{2}(1 + \cos^2\theta)\sigma_1(\omega), \quad (7)$$

with θ being the angle between the pump polarization and the direction of propagation of the circularly polarized probe.

For experiments carried out in a 1D optical molasses configuration with counterpropagating σ^+ and σ^- beams of equal intensity, the light polarization is linear locally (ignoring extinction due to scattering). Depending on the geometry and probe polarization, the measured cross section is given by either Eq. (6) or (7) averaged properly over θ [9]. In the experiment of [3], the probe beam is

circularly polarized and is propagating (approximately) along the axis of the pumping beams. In this case $\theta = \pi/2$ in Eq. (7) and we have $\sigma(\omega) = [\sigma_0(\omega) + \sigma_1(\omega)]/2$. Figure 1 shows our result for the cycling transition of Cs. It can be compared to Figs. 1(a) and 1(b) of [3]. We have taken $\gamma/2\pi = 5.28$ MHz which is calculated, using angular-momentum algebra, from the experimental value of 6.36 a.u. for the reduced dipole matrix element between $6s_{1/2}$ and $6p_{3/2}$ [10]. $\Delta/2\pi = -10.6$ MHz is the experimental condition of [3]. $\Omega_{eg}/2\pi = 52.4$ MHz corresponds to an intensity of 10 mW/cm² for each of the pumping beams. The agreement between theory and experiment is quite satisfactory. The differences, including the much narrower ‘‘Rayleigh’’ resonance, can be attributed to the effects of atomic motion, which we have ignored. The treatment of these effects is nontrivial and open to further investigation [3–5]. Figure 2 shows the underlying $\sigma_0(\omega)$ and $\sigma_1(\omega)$ over a much wider frequency range. Note that only σ_1 ($=\sigma_{-1}$) has a narrow structure around $\omega = \omega_L$, consistent with the interpretation that it is due to the stimulated Raman processes [2]. Our argument for such an interpretation is as follows. Since these structures are so narrow (in fact they can be infinitely

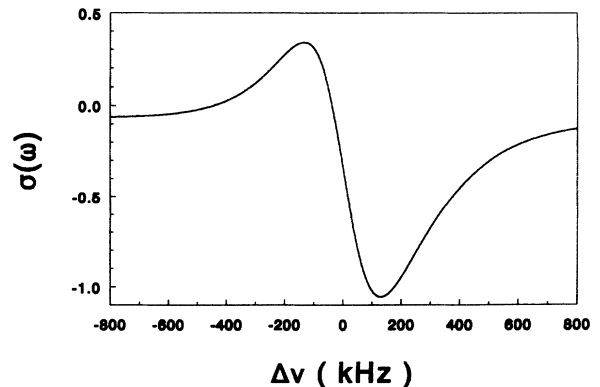


FIG. 1. Net gain cross section, in units of $\pi(\lambda_{eg}/2\pi)^2 = 5.78 \times 10^{-10}$ cm², for the cycling transition of Cs vs $\Delta\nu \equiv (\omega - \omega_L)/2\pi$. $\gamma/2\pi = 5.28$ MHz; $\Delta/2\pi = -10.6$ MHz; and $\Omega_{eg}/2\pi = 52.4$ MHz.

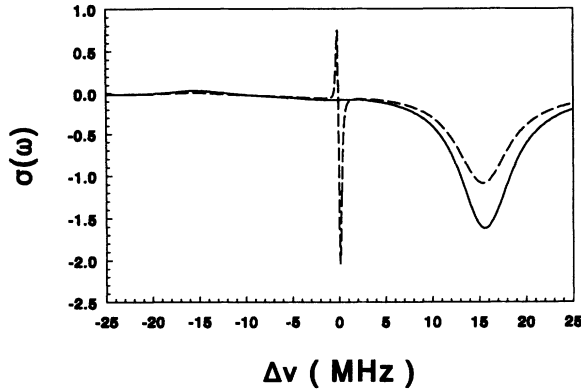


FIG. 2. Same as Fig. 1 except both σ_0 (solid line) and σ_1 (dashed line) are shown over a much greater frequency range.

narrow theoretically), they have to be the results of processes among ground-state Zeeman sublevels, in which excited states play only the role of intermediate states. This is because any processes involving the excited state as either the initial or final state would invariably have a width of the order of γ . Now since stimulated Raman transitions are the only processes of this type contained in $\sigma_{\pm 1}$, they have to be responsible for the narrower structures in them. Another type of processes among ground-state Zeeman sublevels is the stimulated Rayleigh transitions, whose contribution to the probe spectrum is contained solely in σ_0 . Our calculations show that they do not give rise to any *narrow* structures (see also other examples). We therefore conclude that ignoring atomic motion, all narrow structures in the weak probe spectrum come from stimulated Raman processes. Widths of these structures are induced by the pump laser field and are proportional to Ω_{eg}^2 in the limit of weak pump-atom coupling [11,12]. For strong pump-atom couplings, these structures gradually broaden and eventually become part of a spectrum in which every structure has a width of the order of γ . For this reason and for more direct comparison with perturbation theories, we will now focus ex-

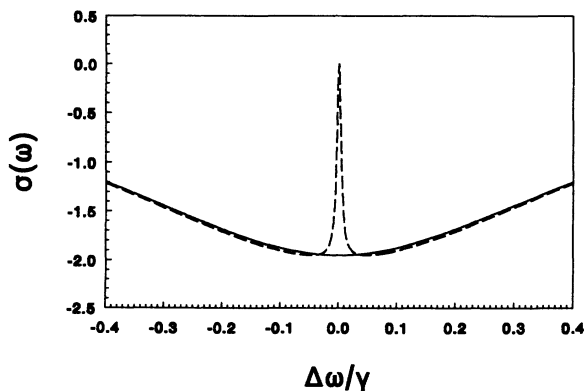


FIG. 3. Net gain cross section, in units of $\pi(\lambda_{eg}/2\pi)^2$, for a $\frac{1}{2}$ transition vs $\Delta\omega/\gamma \equiv (\omega - \omega_L)/\gamma$. $\Delta=0$ and $\Omega_{eg}=0.2\gamma$. Solid line: σ_0 ; dashed line: σ_1 .

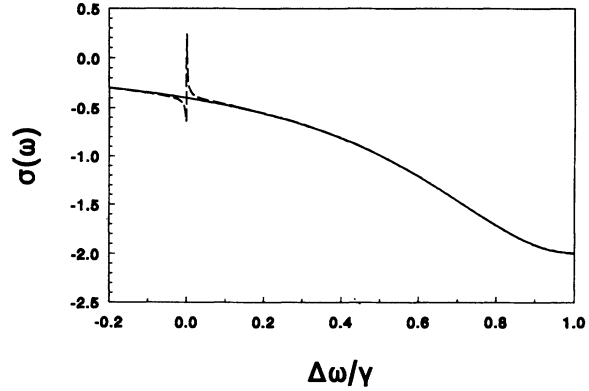


FIG. 4. Same as Fig. 3 except for $\Delta = -1\gamma$.

clusively on the case of weak pump-atom coupling. It should, however, be pointed out that all figures in this paper are calculated by a single program that applies to arbitrary angular momentum, detuning, and Rabi frequency. No specific approximations are made in generating any of them. Also, the meaning of the *weak* pump-atom coupling has to be understood within the context of our theory which always requires the pump field to be much stronger than the probe field.

Figures 3–5 show the results for a $J_e = J_g = \frac{1}{2}$ transition with $\Omega_{eg} = 0.2\gamma$ and three different detunings. For this transition, an analytic expression for the spectrum can be easily derived using the method of [8]. It is most instructive to see only the part that gives the line shape for the *narrow structure* in σ_1 in the limit of weak pump-atom coupling, for which we obtain

$$\begin{aligned} \sigma_1(\omega) = & -2(\gamma/2)^2[\Delta^2 + (\gamma/2)^2]^{-1} \\ & + 2(\gamma/2)^2[\Delta^2 + (\gamma/2)^2]^{-1} \frac{r^2}{(\omega - \omega_L)^2 + r^2} \\ & - \gamma\Delta[\Delta^2 + (\gamma/2)^2]^{-1} \frac{r(\omega - \omega_L)}{(\omega - \omega_L)^2 + r^2}, \end{aligned} \quad (8)$$

where

$$r = \gamma[1 - (2J_e + 1)f_m^2](f_m\Omega_{eg}/2)^2[\Delta^2 + (\gamma/2)^2]^{-1}, \quad (9)$$

with $m = \frac{1}{2}$. Note that r is the spontaneous Raman

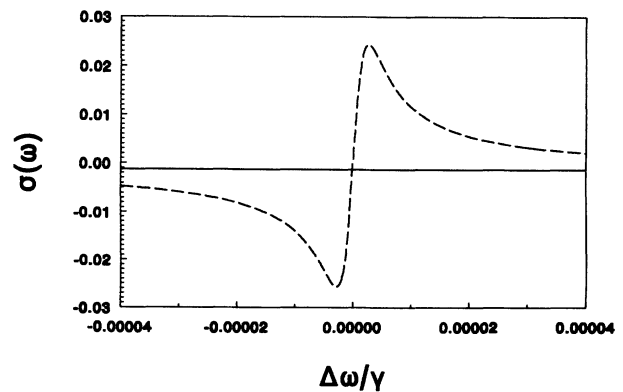


FIG. 5. Same as Fig. 3 except for $\Delta = -20\gamma$.

scattering rate out of either $m_g = \frac{1}{2}$ or $m_g = -\frac{1}{2}$ state. The first term in Eq. (8) describes the background due to the usual absorption. The other two terms describe the line shape of the narrow resonance which is due to the stimulated Raman scattering between $m_g = \frac{1}{2}$ and $m_g = -\frac{1}{2}$. Unlike the narrow structures in Figs. 1 and 2, which are combined results of many resonances, the narrow structure of Eq. (8) is a single resonance. The results of Figs. 3–5 are interesting for a number of reasons. Figure 3 tells us for example that complete transparency of a linearly polarized probe beam can be achieved right on the atomic resonance ($\omega = \omega_{eg}$) by using a weak pumping beam with the same frequency and a linear polarization perpendicular to the probe polarization [$\sigma = \sigma_1$ from Eq. (6)]. This turns out to be true for all transitions with $J_e = J_g$ and equal to half integers (we tested it explicitly for $J_g = \frac{1}{2}, \frac{3}{2}, \frac{5}{2}, \frac{7}{2}$, and $\frac{9}{2}$ transitions). Under the same conditions, the narrow structure for transitions with $J_e = J_g + 1$ and J_g being an integer is a dip at $\omega = \omega_L = \omega_{eg}$, leading to extra absorption. Figure 6 illustrates this point for a 2 to 3 transition. The type of behaviors we are seeing in Figs. 3 and 6 can be useful for frequency filtering and precision spectroscopy. Figures 4 and 5 represent the spectra of the $\frac{1}{2}$ to $\frac{1}{2}$ transition at intermediate and large detunings. In the limit of large detuning ($|\Delta| \ll \gamma$), the line shape becomes purely dispersive (Fig. 5) and is described by the third term of Eq. (8).

Grynberg, Vallet, and Pinard [13] have considered the $\frac{1}{2}$ to $\frac{1}{2}$ transition in the configuration of orthogonal linear polarizations [$\sigma = \sigma_1$ from Eq. (6)]. Their result, derived in the limit of large detuning, agrees with the third term of Eq. (8), and is thus the stimulated Raman resonance between $m_g = \frac{1}{2}$ and $m_g = -\frac{1}{2}$. This resonance sits right on $\omega = \omega_L$ simply because a linearly polarized pump field cannot lift the degeneracy between $m_g = \frac{1}{2}$ and $m_g = -\frac{1}{2}$ states. The question of whether the stimulated Rayleigh scattering would give rise to narrow resonances is not relevant here. Since the probe photon has no $q = 0$ component, the combination of one probe photon and any number of pump photons can never return the atom to the same m state; i.e., the stimulated Rayleigh scattering cannot happen in the configuration of linear orthogonal

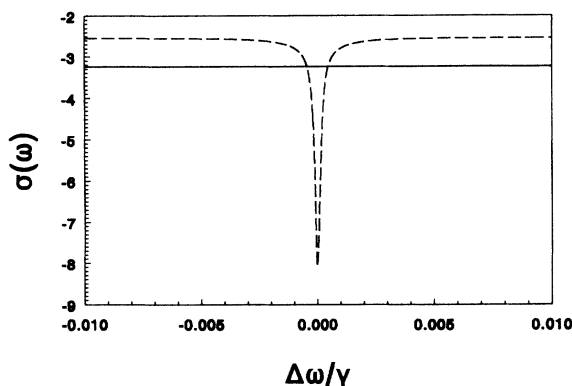


FIG. 6. Same as Fig. 3 except that it is for a $J_g = 2$ to $J_e = 3$ transition.

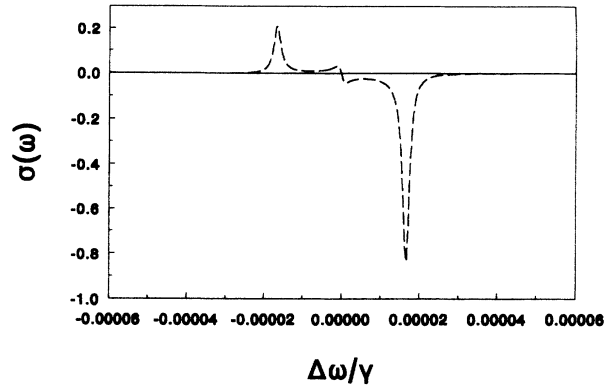


FIG. 7. Net gain cross section, in units of $\pi(\lambda_{eg}/2\pi)^2$, for a $\frac{3}{2}$ to $\frac{5}{2}$ transition vs $\Delta\omega/\gamma \equiv (\omega - \omega_L)/\gamma$. $\Delta = -20\gamma$ and $\Omega_{eg} = 0.2\gamma$. Solid line: σ_0 ; dashed line: σ_1 .

polarizations [14]. Such an interpretation is further supported by the observation that while all half-integer transitions have a purely dispersive feature at $\omega = \omega_L$ in the limit of large detuning, transitions with integer angular momentum do not have it in the same limit. This is illustrated in Figs. 7 and 8, which show the results for a $\frac{3}{2}$ to $\frac{5}{2}$ transition and a 1 to 2 transition, respectively.

Results such as Figs. 3–5 and 7 are hard to understand from the traditional wave-function perturbation theory. For half-integer transitions, the populations in $m_g = -\frac{1}{2}$ and $m_g = +\frac{1}{2}$ are always equal [8]. Wave-function perturbation theory, which is normally expected to be valid in the limit of weak pump-atom coupling, would predict a zero cross section for the stimulated Raman scattering between $m_g = -\frac{1}{2}$ and $m_g = +\frac{1}{2}$. To understand this apparent contradiction, we have only to realize that the wave-function perturbation theory is intrinsically deficient in predicting line shapes for transitions between bound states. From some transition amplitude T_{if} , it tells us that the transition rate is given by something like $(2\pi/\hbar)|T_{if}|^2\delta(\omega - \omega_0)$, which is of course not the correct line shape for anything but the coherent Rayleigh scattering. All we can expect from it is therefore to get the in-

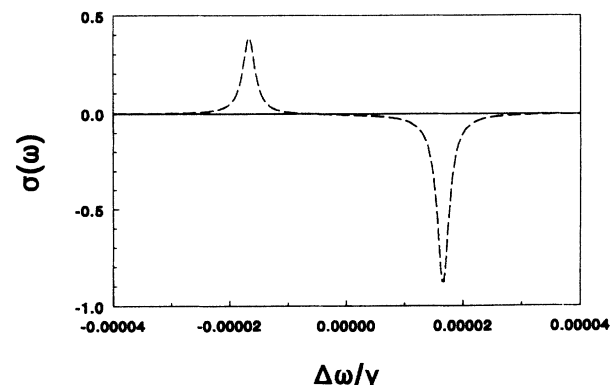


FIG. 8. Same as Fig. 7 except that it is for a $J_g = 1$ to $J_e = 2$ transition.

egrated rate right. Indeed it can be shown from Eqs. (3) and (4) that the wave-function perturbation theory does do its job in predicting the integrated rates. In fact, in the limit of large detuning where all lines are split, it can even get the *integrated* rates of *individual* lines right. For example, the integrated rate of the purely dispersive feature is zero, in agreement with the prediction of the wave-function perturbation theory, which also helps us understand the following interesting feature of the probe spectrum. After the detuning has become sufficiently large so that all lines are split (as is the case in Figs. 7 and 8), the heights of all resonances except the purely dispersive structure remain the same upon further increase of detuning or further decrease of pump intensity. The whole spectrum simply gets squeezed to a smaller scale. This is because the perturbative rates for stimulated Raman scatterings, which are related to the integrated cross sections over individual resonances, depend on the detuning and Rabi frequency in the same way as the rates that determine the widths [12].

Finally, the line shape given by Eq. (8) is obviously nonperturbative in the sense that it cannot be expanded in a power series of Ω_{eg} . It therefore could not have been obtained from even the usual density-matrix perturbation theory [15] which works fine for a two-level system. This nonperturbative nature is related intimately to the fact that in the absence of any pump field (and ground-state m -changing collisions), an atom with a degenerate ground state does not have a unique steady state. Its Liouville operator has multiple eigenstates corresponding to the eigenvalue zero. What happens then is similar to what happens to degenerate energy levels under an external perturbation [11,4,5]. (Remember that the degenerate perturbation theory is nonperturbative as far as coupling among degenerate states is concerned.) This is the most important difference between atoms with and without a ground-state degeneracy.

I am deeply indebted to Jinx Cooper for getting me interested in this problem and for helpful discussions.

-
- [1] J. W. R. Tabosa, G. Chen, Z. Hu, R. B. Lee, and H. J. Kimble, *Phys. Rev. Lett.* **66**, 3245 (1991).
- [2] D. Grison, B. Lounis, C. Salomon, J. Y. Courtois, and G. Grynberg, *Europhys. Lett.* **15**, 149 (1991).
- [3] B. Lounis, J. Y. Courtois, P. Verkerk, C. Salomon, and G. Grynberg, *Phys. Rev. Lett.* **69**, 3029 (1992).
- [4] J. Guo and P. R. Berman, *Phys. Rev. A* **47**, 4128 (1993).
- [5] J. Y. Courtois and G. Grynberg, *Phys. Rev. A* **48**, 1378 (1993).
- [6] M. Trippenbach, B. Gao, and J. Cooper, *Phys. Rev. A* **45**, 6555 (1992).
- [7] C. Cohen-Tannoudji, in *Frontiers in Laser Spectroscopy*, edited by R. Balian, S. Haroche, and S. Liberman (North-Holland, Amsterdam, 1977), p. 3.
- [8] B. Gao, *Phys. Rev. A* **48**, 2443 (1993).
- [9] We have assumed that the medium is optically thin so that the change of probe polarization can be ignored. This is apparently the case for the experiment of [3]. Generalization to other cases is obvious.
- [10] L. Shabanova, Yu. Monukov, and A. Khlyustalov, *Opt. Spektrosk.* **47**, 3 (1979) [*Opt. Spectrosc. (USSR)* **47**, 1 (1979)].
- [11] P. R. Berman, *Phys. Rev. A* **43**, 1470 (1991) and references therein.
- [12] B. Gao (unpublished).
- [13] G. Grynberg, M. Vallet, and M. Pinard, *Phys. Rev. Lett.* **65**, 701 (1990).
- [14] If one really wants to probe the stimulated Rayleigh scatterings, the parallel linear polarizations would be the ideal configuration ($\sigma = \sigma_0$ in this case and therefore no contamination from stimulated Raman transitions). Our theory predicts that no *narrow* features would be seen in this configuration.
- [15] G. Grynberg and P. R. Berman, *Phys. Rev. A* **39**, 4016 (1989) and references therein.